China Ocean Engineering, Vol.17, No.4, pp.589 – 604

Numerical Study on Breaking Criteria for Solitary Waves*

Chung-ren CHOU[a], Ruey-syan SHIH[b,1] and John Z. YIM[a]

[a] *Department of Harbor and River Engineering, Taiwan Ocean University, Keelung, China*

[b] *Department of Civil Engineering, Tung Nan Institute of Technology, Taipei, China*

(Received 12 October 2002; accepted 30 June 2003)

ABSTRACT

Studies of the breaking criteria for solitary waves on a slope are presented in this paper. The boundary element method is used to model the processes of shoaling and breaking of solitary waves on various slopes. Empirical formulae that can be used to characterize the breaking of solitary waves are presented. These include the breaking index, the wave height, the water depth, and the maximum particle velocity at the point of breaking. Comparisons with the results of other researches are given.

Key words: *boundary element*; *breaking indices*; *empirical formula*; *solitary wave*

1. Introduction

Although wave breaking is commonly observable, yet is it one of the most complicated occurrences of nature. Studies on wave breaking are important both for physical oceanographers and ocean engineers. When waves are breaking, turbulence eddies will be generated, which on their side will intensify the exchange of gases, moisture, and particles with the atmosphere. On the other hand, the large pressure associated with broken waves can be devastating. Understanding the characteristics and the mechanism of wave breaking are essential for engineers, as this can help to avoid destructions of coastal structures and to protect human lives.

Thorough investigation on the properties of breaking waves and arrangement of unequivocal results of their effects are by no means facile, and are still one of the extensively studied subjects in the field of ocean engineering nowadays. Since in the fifties of the last century, researchers have used flow visualization techniques to study the properties of waves at breaking. They have studied the possible height, the water depth, the crest angle, the location, as well as the velocities of water particles and their trajectories of breaking waves. Experimental formulae for coastal engineering applications have been recommended. Ippen and Kulin (1955), for instance, (see also Street and Camfield, 1966; Saeki *et al.*, 1971) investigated the variations of wave heights, the water depths, and the run-up heights of breaking waves during the breaking processes through laboratory measurements.

Through these efforts, empirical formulae regarding the characteristics of breaking waves were proposed. These equations are ready for engineering applications. However, accurate measurements of a breaking wave field are very difficult. This is true even for controlled experiments such as those in the

* The work was financially supported by the Taiwan Science Council (Project No. NSC-89-2611-E-019-064)

1 Corresponding author, E-mail: rsshih@mail.tnit.edu.tw

laboratories. As a result, only quantitative descriptions of a breaking wave field can be given. On the other hand, it is interesting, both academically as well as practically, to have detailed studies of the interior of the breaking wave field. To have a thorough understanding of this complicated phenomenon, one would have to know the velocity and acceleration of the water particles and the transformation of energy within the wave field.

One way to obtain this information is to use highly modern, albeit expensive, measuring techniques. Trizna *et al*. (1999), for example, have studied the steep and complex crest structure of a spilling breaker in laboratory. The high speed CCD camera was operated at 6000 frames per second to estimate the influence of surface fluctuations. Alternatively, laser-Doppler anemometers (LDA) were also used for the study of the velocity field of breaking waves. Another way to study the complicated process of wave breaking is through numerical modelling. Numerical models with various solution techniques have been implemented to model variations of the waveform, as well as the internal flow field.

Koshizuka *et al*. (1998) (see also Gotoh and Sakai, 1999), for example, used the moving particle semi-implicit (MPS) method to simulate the process of wave breaking. When the Lagrangian concepts are used to a fluid (Lagrangian approach), they can be used to simulate fluid-structure interactions with large boundary movement. Dommermuth *et al*. (1988) found that high-wavenumber instabilities will occur at the free surface in simulating the process of wave breaking. To avoid this problem, special treatment such as smoothing can be used. On the other hand, it should be pointed out that, even though the accumulation of errors can be reduced effectively through smoothing, excessive adjustment would also diminish the accuracy of the numerical scheme. Dommermuth and Yue (1987) implemented a regridding algorithm that effectively removes the instabilities without causing additional problems at the intersection points, as was the case when smoothing is used.

Grilli *et al*. (1996, 1997) reduced the errors in mass and energy by improving the resolution in breaker jet through addition and regridding of the discretization nodes. This technique allows their computations to be pursed beyond the breaking point until the jets almost touch down on the free surface, the waveform at breaking can thus be described perfectly and stably. However, some of their results appeared to be unrealistic because they do not conform to the natural phenomena. For example, breaking wave heights sometimes exceeded 8 or 9 times of the water depth, and approached excessively close to the coastline.

It may be pointed out that, in comparison with empirical results, formulae for breaker type, breaking index, the wave height and water depth at breaking, as obtained through numerical investigations, are still limited. In this paper, a numerical model is presented, with the boundary element method used to study the characteristics of solitary waves as they break on slopes. Empirical formulae will be presented and compared with the results published previously by other researchers.

2. Numerical Modeling and Simulations

In this paper, the process of propagation and breaking of solitary waves is solved with boundary element method. Fig. 1 shows the sketch of a numerical wave tank confined in a region composed of:

a moving wave-making paddle, an undisturbed free water surface, an impermeable slope, and an impermeable seabed. The fluid within the region is assumed to be inviscid and incompressible and the flow is irrotational. Boundaries in the regime of the numerical analyses are discretized with linear elements.

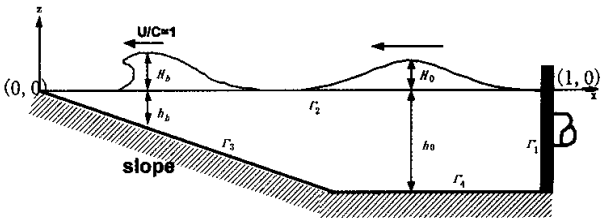

Fig. 1. Definition sketch of numerical wave tank.

The continuity equation is solved with the linear boundary element method based on the Green's second identity, where the velocity potential satisfies the following Laplace equation:

$$\frac{\partial^2 \Phi}{\partial x^2} + \frac{\partial^2 \Phi}{\partial z^2} = 0. \tag{1}$$

2.1 Boundary Conditions

(1). Boundary conditions on the free water surface

Boundary conditions on the undisturbed free water surface can be obtained from the nonlinear kinematic and dynamic conditions and are expressed as:

$$u = \frac{\mathrm{D}x}{\mathrm{D}t} = \frac{\partial \Phi}{\partial x}; \tag{2}$$

$$w = \frac{\mathrm{D}z}{\mathrm{D}t} = \frac{\partial \Phi}{\partial z}; \tag{3}$$

$$\frac{\mathrm{D}\Phi}{\mathrm{D}t} + g\zeta - \frac{1}{2}\left[\left(\frac{\partial \Phi}{\partial x}\right)^2 + \left(\frac{\partial \Phi}{\partial z}\right)^2\right] = 0; \tag{4}$$

where $\mathrm{D}/\mathrm{D}t$ is the Lagrange differentiation, g is the gravitational acceleration, and ζ is the surface elevation.

(2). Boundary conditions on the impermeable slopes and seabed

The water particle velocity is null in the normal direction on the impermeable seawall and seabed, therefore the condition is prescribed as:

$$\frac{\partial \Phi}{\partial n} = 0, \quad \text{on } \Gamma_3 \text{ and } \Gamma_4 \tag{5}$$

in which n is unit outward normal vector.

(3). Boundary condition on the pseudo wave paddle

In this study a piston type wavemaker is used to generate waves with prescribed property. On the surface of the wave paddle, continuity of the horizontal velocities of the wave-paddle and that of the fluid flow lead to:

$$\bar{\Phi} = \frac{\partial \Phi}{\partial n} = -U(t). \tag{6}$$

For solitary waves, according to the Boussinesq equation, $U(t)$ can be expressed as:

$$U(t) = H_0\sqrt{\frac{g}{h}} \cdot \sec h^2\left[\sqrt{\frac{3H_0}{4h^3}}C(t - t_c)\right] \tag{7}$$

where H_0, h, and C are, respectively, the incident wave height, the water depth, and the wave celerity; t_c is a characteristic time scale, which is defined as half the time of the stroke of the wave paddle.

The pseudo wave paddle should be placed at a distance greater than L_{eff} from the origin of coordinate, where L_{eff} is the effective wavelength (Tsusaka, 1983) for solution given as:

$$L_{eff} = 9.5766h\sqrt{\frac{h}{\zeta_0}}. \tag{8}$$

This definiendum is treated as the wavelength L_0 of solitary wave thereinafter. ζ_0 denotes the amplitude (elevation) of the incident solitary wave.

2.2 Governing Equations

In this sub-section, a brief description will be given of the governing equations and the applied numerical scheme. Detailed descriptions can be found in Chou and Shih (1996a). According to Green's second identity, the velocity potential $\Phi(x, z; t)$ within the region can be obtained by the velocity potential on the boundary, $\Phi(\xi, \eta; t)$, and its normal derivative, $\partial\Phi(\xi, \eta; t)/\partial n$, thus,

$$\Phi(x, z; t) = \frac{1}{2\pi}\int_\Gamma\left[\frac{\partial\Phi(\xi, \eta; t)}{\partial n}\ln\frac{1}{r} - \Phi(\xi, \eta; t)\frac{\partial}{\partial n}\ln\frac{1}{r}\right]\mathrm{d}s \tag{9}$$

with $r = [(\xi - x)^2 + (\eta - z)^2]^{1/2}$.

When the inner point $(x, z; t)$ approaches the boundary point $(\xi', \eta'; t)$, Eq. (9) is expressed through:

$$\Phi(\xi', \eta'; t) = \frac{1}{\pi}\int_\Gamma\left[\frac{\partial\Phi(\xi, \eta; t)}{\partial n}\ln\frac{1}{R} - \Phi(\xi, \eta; t)\frac{\partial}{\partial n}\ln\frac{1}{R}\right]\mathrm{d}s \tag{10}$$

where $R = [(\xi - \xi')^2 + (\eta - \eta')^2]^{1/2}$.

As shown in Fig. 1, the boundaries Γ_1 through Γ_4 are divided into N_1 to N_4 discrete segments with linear elements for calculation. Hence, Eq. (10) can be expressed more compactly in a matrix form:

$$[\Phi_i] = [O_{ij}][\bar{\Phi}_i], \quad i, j = 1 \sim 4 \tag{11}$$

where $[\Phi]$ and $[\bar{\Phi}]$ are the nodal values of the potential function and its normal derivative on the boundaries, respectively, and $[O]$ is a matrix related to the geometrical shape of the boundaries. Detailed expressions of these matrixes can be found in Chou and Shih (1996a).

The stability of the model has been discussed in detail by Chou and Shih (1996a, 1996b) previously, including in the simulation of both solitary waves and periodical waves, and the conservative property of the numerical scheme is cross-checked by the continuum equations for mass and energy, which demonstrated that our results are consistent with theoretical ones.

2.3 Numerical Simulation

The length of the wave flume and the number of discrete elements differ from case to case. Take the case of slope = 1 :50 for example, as shown in Fig. 2, the total length of the wave flume is 70 meters. The boundaries Γ_1 through Γ_4 are divided respectively into $N_1 = 10$, $N_2 = 153$, $N_3 = 200$, and $N_4 = 80$ dicrete elements. Notice that the elements on the surface are not of uniform size, and the spatial resolutions are varied, for they are divided into six systems, as shown in the figure. Coarser meshes are used at both ends of the flume, and are then varied gradually when approaching the slope where the waves might breaks, i.e. $\Delta s = 1\ h$, $\Delta s = 0.5\ h$, $\Delta s = 0.5\ h \sim 0.25\ h$, $\Delta s = 0.2\ h$, $\Delta s = 0.25 \sim 0.5\ h$, and $\Delta s = 0.5\ h$, for a purpose to simulate the breaking wave more authentically. On the other hand, in order to save computer storage and computation time, several temporal resolutions are used during computation: resolution of $\Delta t = t_c/200$ is used for $0 \sim 2.5$ seconds, resolution of $\Delta t = t_c/500$ is used for $2.5 \sim 4.4$ seconds, and resolution of $\Delta t = t_c/1000$ is used for 4.4 seconds till breaking.

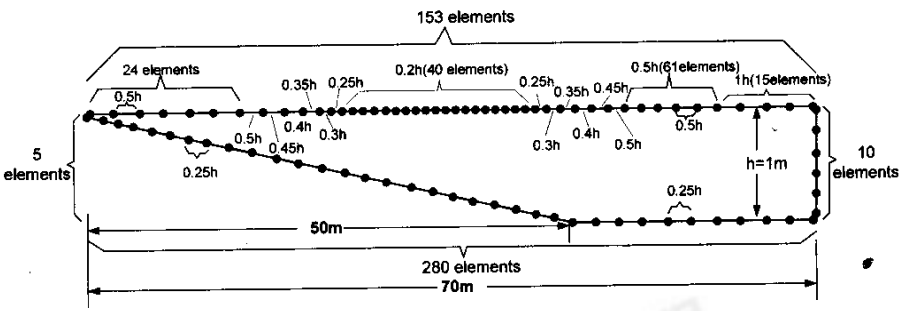

Fig. 2. Discretization scheme for slope = 1 :50.

3. Results and Discussions

3.1 Breaking Criteria

It is well known that wave breaking may depend on various factors such as wave steepness, wave height, and beach slope. Battjes suggested that the so-called Irribarren number, also known as surf similarity parameter, could be used as a criterion. Chou and Ouyang (1999a, 1999b) discussed the criterion for breaking of solitary waves on slopes in some detail. They found that breaking occurs when the condition of $u/C \approx 1$ is satisfied, u being average horizontal velocities of water particles near the crest and C, wave celerity calculated through:

$$C = \sqrt{gh} \cdot \left[1 + \frac{1}{2}\left(\frac{H}{h}\right) - \frac{1}{8}\left(\frac{H}{h}\right)^2 + \frac{1}{16}\left(\frac{H}{h}\right)^3 - \frac{5}{128}\left(\frac{H}{h}\right)^4\right]. \quad (12)$$

Additionally, the condition when part of the wave front has become vertical can also be considered as a criterion for breaking. These criteria are adopted for further discussion in this study.

Breaking waves are traditionally classified as spilling, plunging, and surging breakers according

to their appearances. Occasionally, the term collapsing is also used to denote breaking waves that lie between plunging and surging breakers (See, e.g., Galvin, 1968). In this study, numerical results are divided into four categories. These are: waves that are not breaking, plunging breakers accompanied with run-up, plunging breakers, and spilling breakers. The difference between "breaking with run-up" and "plunging breakers" is the occurrence of the shifting shoreline. In other words, since the shoreline shifts as a non-breaking wave runs up the beach, and a plunging breaker collapses before approaching the shore. Breakers that possess simultaneously the characteristics of shifting shoreline and breaking are therefore defined as "breaking with run-up".

In modeling of the complicated process of wave breaking, which is highly nonlinear by nature, it is quite difficult to pursue computation beyond the breaking point. Quite often, it is found that mass and energy are not conserved due to accumulated errors during computation. This was improved by Grilli *et al*. (1997) by increasing and refining the discretization nodes. This technique allowed them to pursue their computations beyond the breaking point. In fact, some of their results show the touchdowns of the breaker jets on the free surface. It can be seen that in most of their numerical results water jets have appeared.

As mentioned above, $u/C = 1$ is used as the criterion for wave breaking in this paper. In Table 1, a number of our numerical results are compared with those of Grilli *et al*. (1997). These include the dimensionless breaking wave height, H_b/h_0, the relative breaking wave height, H_b/h_b, and the dimensionless depth of breaking wave, h_b/h_0. In all of the above notations, H is the wave height, h is the water depth, and the subscripts 0 and b denote the conditions of the initial state, and at the breaking point, respectively.

Table 1 Comparison between present results and those of Grilli *et al*. (1997)

Slope	H_0/h_0	H_b/h_b		H_b/h_0		h_b/h_0	
		Chou	Grilli	Chou	Grilli	Chou	Grilli (* exp.)
1:15	0.30	1.688	2.651	0.407	0.398	0.241	—
1:20	0.20	1.636	2.104	0.334	0.332	0.204	—
1:35	0.10	1.240	1.950	0.210	0.203	0.169	0.100
1:35	0.15	1.336	1.473	0.330	0.296	0.247	0.177
1:35	0.20	1.330	1.402	0.402	0.364	0.302	0.252
1:35	0.25	1.314	1.385	0.465	0.422	0.354	0.300
1:35	0.30	1.283	1.380	0.514	0.476	0.400	—
1:35	0.40	1.260	1.378	0.614	0.592	0.487	—

3.2 Predictions of Breaking Criterion and Breaking Characteristics

3.2.1 *Breaking Criterion and Breaker Type*

Researchers have always been interested in finding a clear definition for the breaking criterion, as

well as the breaker type, for solitary waves on uniform slopes (see e.g., Galvin, 1968; Weggel, 1972; Battjes, 1974). Battjes suggested that the surf similarity parameter could be used as an indication of how the waves break. However, the physics, as well as the characteristics, of a solitary wave before and after breaking are entirely different as compared with those of a group of waves with harmonic components. This is because the former has only one single wave crest, and, therefore, the possible influences of the backwash aroused by previous broken waves will not occur. To determine the breaker type adopted in this study, we utilize not only the variations of static waveform shown in related figures but also the dynamic view from a special browser for more conclusive confirmation. Estimated breaker types in accordance with various slopes and dimensionless wave heights are tabulated in Table 2. The abbreviations such as NB, PR, PL, and SP denote, respectively, non-breaking, plunging with runup, plunging, and spilling breakers.

Table 2 Estimations of breaker types corresponding to various slopes

	Slope												
H_0/h_0	1:2.5	1:5	1:7.5	1:10	1:12.5	1:15	1:20	1:25	1:30	1:35	1:40	1:45	1:50
0.05	NB	NB	NB	NB	NB	NB	NB	NB	NB	NB	NB	NB	NB
0.10	NB	NB	NB	NB	NB	NB	PL	PL	NB	PL	PL	SP	SP
0.15	NB	NB	NB	PR	PR	PR	PR	PL	PL	PL	PL	SP	SP
0.20	NB	NB	NB	PR	PL	PL	PL	PL	PL	PL	SP	SP	SP
0.25	NB	NB	NB	PR	PL	PL	PL	PL	PL	PL	SP	SP	SP
0.30	NB	NB	PR	PR	PL	PL	PL	PL	SP	PL	SP	SP	SP
0.35	NB	NB	PR	PL	PL	PL	PL	SP	SP	SP	SP	SP	SP
0.40	NB	NB	PR	PL	PL	SP	SP	SP	SP	SP	SP	SP	SP

Notes: H_0 is the incident wave height, and h_0 is the deepwater depth.

The above results are also plotted in Fig. 3. The limit between the "non-breaking" and "plunging breaker with run-up" is estimated at:

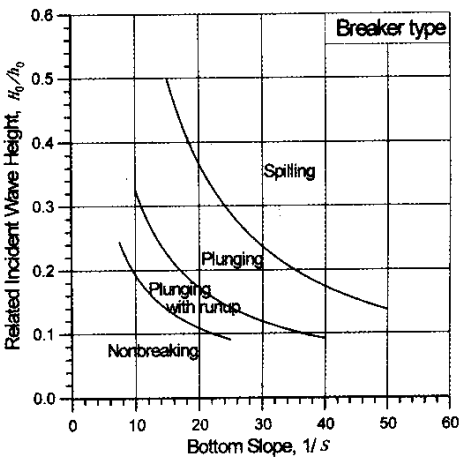

Fig. 3. Estimations of breaker types corresponding to various slopes and related incident wave heights.

$$\frac{H_0}{h_0} = 1.295S^{0.828} \tag{13}$$

where H_0/h_0 and S denote the relative incident wave height and the bottom slope, respectively. In other words, the breaking criterion can be determined as:

$$\frac{H_0}{h_0} > 1.295S^{0.828}. \tag{14}$$

A similar criterion for the non-breaking and breaking waves was also given by Grilli *et al*. (1997) as $H_0/h_0 > 16.9S^2$ by use of a least-square method. Using nonlinear shallow water equations, Synolakis (1987) found that the limit for waves to break when running up a slope can be expressed as $H_0/h_0 > 0.818S^{10/9}$. These empirical relations are plotted in Fig. 4 for comparison, where the broken lines are those from the two previous studies.

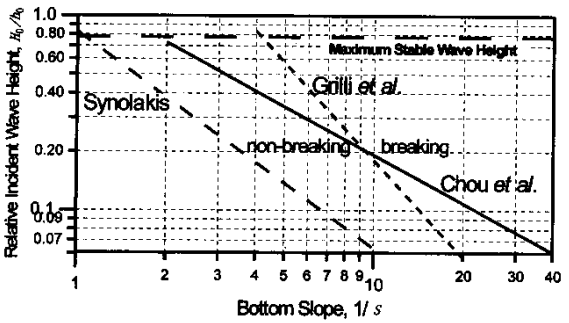

Fig. 4. Comparison between the present wave-breaking criterion for solitary waves on slopes and that of Grilli *et al*. (1997) and Synolakis (1987).

The phrase" plunging with run-up "is used in this study to denote the cases when the characteristics of both plunging and run-up can be clearly seen from calculated results. As can be seen from Table 1, this type of breaker occurs in a very narrow range depending on bottom slopes, which is estimated to be

$$1.295S^{0.828} < \frac{H_0}{h_0} < 2.684S^{0.917}. \tag{15}$$

It was mentioned earlier that plunging breakers occur mainly on steeper beaches when the wave heights are small and the wavelengths are long. Using Fig. 3, a criterion for plunging breakers to occur can be obtained as:

$$2.684S^{0.917} < \frac{H_0}{h_0} < 9.2S^{1.076}. \tag{16}$$

Similarly, on varying mildly sloping beaches, the criterion for spilling breaker is determined as:

$$\frac{H_0}{h_0} > 9.2S^{1.076}. \tag{17}$$

It can be seen from Fig. 4 that, when $H_0/h_0 > 0.2$ our results are located between those of Gril-

li *et al*. and Synolakis; whereas for smaller dimensionless wave heights, $H_0/h_0 < 0.2$, the present results show that waves will break on a slope milder than indicated by the results of the two previous studies.

3.2.2 *Breaking Depth* h_b/h_0

Fig. 5 shows our results of the breaking depth, h_b/h_0, for solitary waves on various slopes. It can be seen from the solid regression line that h_b/h_0 varies from 0.2 to 0.7 for $S_0 < 5$, while it changes from 0.1 to 0.2 for $S_0 > 5$. This shows that, as h_b/h_0 decreases, the breaking point approaches to the coastline, while increasing the value of h_b/h_0 shifts it to the slope toe. Using a least square method for the results of their computations, Grilli *et al*. (1997) expressed the breaking depth as a function of S_0/H_0' through:

$$\frac{h_b}{h_0} = \frac{0.149}{(S_0/H_0')^{0.523}}, \quad \text{with} \quad S_0 < 0.30 \text{ (for SP and PL breakers)}; \tag{18}$$

$$\frac{h_b}{h_0} = \frac{0.0508}{(S_0/H_0')^{1.0}}, \quad \text{with} \quad 0.30 < S_0 < 0.37; S_0/H_0' > 0.385 \text{ (for Surging breaker)}. \tag{19}$$

where H_0' denote the incident wave height, i.e. $H_0' = H_0/h_0$, and S_0 is the ratio of the bottom slope, S, to the relative water depth, h_0/L_0, i.e., $S_0 = S/(h_0/L_0)$. Now, a large value of S_0 indicates that the wave steepness is gentle while the bottom slope is steep. It can be seen from Table 2 that these waves are identified as the NB type, for which S_0 is mostly in the range of $S_0 < 15$. In this study, we have used as conditions for the incident wave heights, $H_0' = 0.1 \sim 0.4$, and for the beach slopes, $S = 0.02 \sim 0.125$, i.e., the slopes have the range of 1:8 ~ 1:50. Therefore h_b/h_0 can be expressed as:

$$\frac{h_b}{h_0} = 0.471 S_0^{-0.502}, \quad \text{with} \quad S_0 \geqslant 0.223. \tag{20}$$

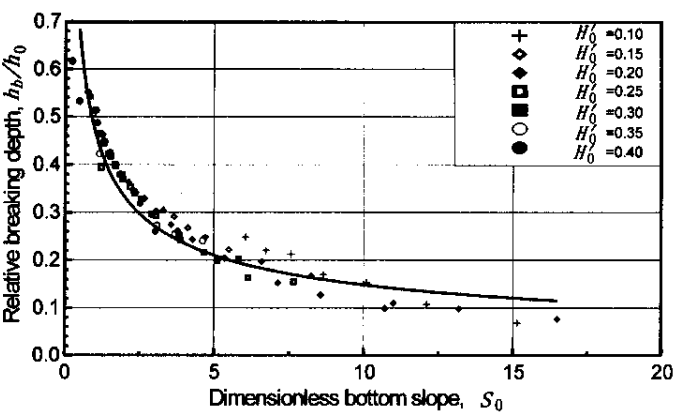

Fig. 5. Regression of breaking depth h_b/h_0 for solitary waves on slopes.

Since $h_b \leqslant h_0$, the right-hand term satisfies $0.471 S_0^{-0.502} \leqslant 1$, i.e. $S_0 \geqslant 0.223$. Substituting various incident wave heights, H_0', into Eq. (20), we have plotted in Fig. 6 some possible curves

for various breaking depths, h_b/h_0, and bottom slopes, S. It can be seen clearly that the breaking wave depths h_b/h_0 for waves on a mild slope are larger than those on a steeper slope. It can also be seen from the figure that, for one and the same inclination, the variations of h_b/h_0 are proportional to H_0', i.e., breaking occurs sooner with a larger incident wave height.

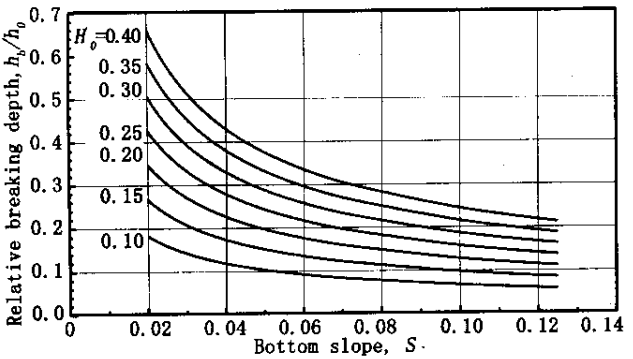

Fig. 6. Relation of the breaking depth for various relative incident wave heights h_b/h_0 and slopes S.

3.2.3 *Breaking Index H_b/h_b*

According to the results of Camfield and Street (1969) (see also Ippen and Kulin, 1995), the upper limit should be 0.78. Though this simple limit has been used as a breaking index for solitary wave breaking over constant depth or very mild slope, in this article, since the slope varies from 1 :2.5 to 1 :50, as mentioned earlier, the breaking criterion for solitary waves on slopes discussed by Chou and Ouyang (1999a,1999b) is used as well.

The relations between the breaking wave height, the breaking wave depth, and the bottom slope can be determined with the experimental formula of Camfield and Street (1968):

$$\frac{H_b}{h_b} = 0.75 + 25S - 112S^2 + 3870S^3. \tag{21}$$

Using a least-square method for their computed results, Grilli *et al*. (1999) determined a breaking index as follows:

$$\frac{H_b}{h_b} = 0.841\exp(6.421S_0). \tag{22}$$

The results of our computation are shown in Fig. 7, where the breaking index can be estimated as:

$$\frac{H_b}{h_b} = 1.590(S_0H_0')^{0.291}. \tag{23}$$

As can be seen from this figure, with a steep bottom slope, i.e., when S_0 is large, or when the relative wavelength is long, i.e., with large L_0/h_0 values, and with $S_0 > 1.5$, the calculated H_b/h_b values are scattered. It is noted that the values of H_b/h_b are relatively large, between 1.5 and 2.5. As shown in Table 2 and Fig. 3, they are classified as the PR type breaker, such as for the cases with $H_0/h_0 = 0.15$ and with the bottom slopes S between 1/10 ~ 1/20.

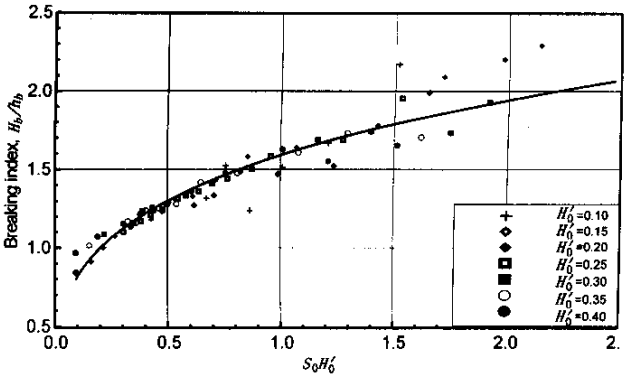

Fig. 7. Regression of breaking index H_b/h_b for solitary wave on slopes.

Fig. 8 shows the results of our computation with Eq. (23). As the bottom slope becomes mild, the type of breaking of a small amplitude solitary wave, i.e., $H_0/h_0 \leqslant 0.15$, will be varied from PR to PL. Since the PR type of breaker is defined to lie between NB and PL breakers, breaking of the PR type will take place at the location closer to the coastline than that of the PL type, thus, the height-to-depth ratio H_b/h_b of the PR breaker will be larger than that of the plunging breaker. It can be seen that, for the PR breaker, H_b/h_b varies from 2.0 to 2.5, whereas for the PL breaker it only varies from 1.4 to 2.0. Similarly, with $H_0/h_0 > 0.15$, the breaker type for solitary waves will change from PL to SP as the bottom slope becomes milder. Similar results can also be seen from the experiments of Yasuda *et al*. (1997). For the same incident wave height, their results show that, when the bottom slope becomes milder, plunging breakers occur closer to the shoreline than spilling breakers. It is therefore clear that the values of H_b/h_b will be larger for waves propagating on steeper slopes than those on milder slopes.

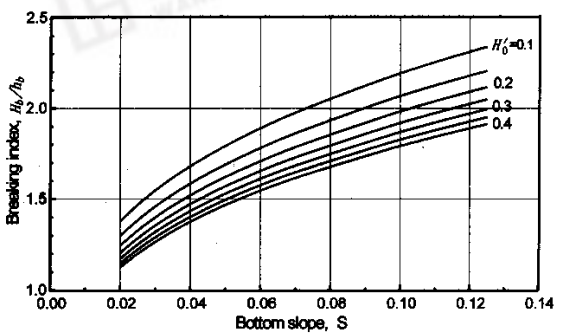

Fig. 8. Relation of breaking index H_b/h_b and bottom slope S for various H_0'.

3.2.4 *Variations of Wave Height* H_b/H_0

As waves approach the surf zone, both the water depth and wave celerity are decreasing as a result of shoaling. Our results are shown in Fig. 9. From the regression curve, the relation between the ratio of breaking wave height to incident wave height H_b/H_0 and the bottom slope S, and the relative water depth h_0/L_0 can be obtained:

$$\frac{H_b}{H_0} = 0.785(S_0 H_0'^3)^{-0.251}. \quad (24)$$

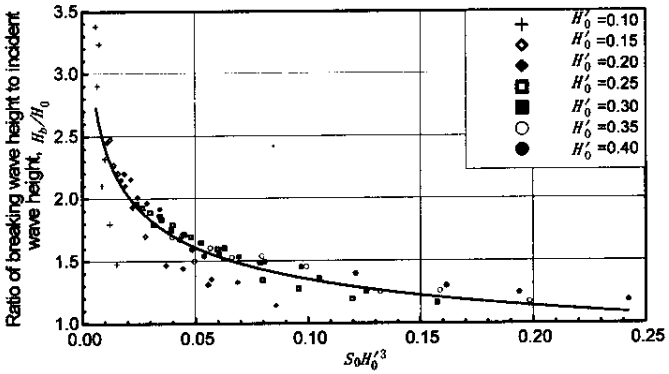

Fig. 9. Comparisons between the wave height variations H_b/H_0 before and after breaking.

Substituting the values of the incident wave height into Eq. (24), the maximum wave heights at breaking can be predicted. Using some incident wave heights, e.g., $H_0/h_0 = 0.10$, 0.15, and 0.20, we have plotted the results in Fig. 10. As can be seen from the figure, when the values of H_0/h_0 is small ($H_0/h_0 = 0.10 \sim 0.20$), the ratios of the breaking wave height to the incident wave height, H_b/H_0, are between $1.7 \sim 2.7$, whereas when H_0/h_0 is large ($H_0/h_0 = 0.25 \sim 0.40$), the change of the value of H_b/H_0 ranges only between $1.1 \sim 1.6$.

3.2.5 *Wave Celerity at Breaking* C_b/C_0

The characteristic of internal flow field of breaking waves in the surf zone is very complicated. Till the present day, it seems that no exact theoretical solution to the phenomenon is available. As a result, the mechanisms have to be studied by laboratory experiments. However, some physical quantities, such as the velocity of fluid particles and the eddy current, are still very difficult to measure.

Ting and Kirby (1994) studied the undertow and turbulence in the surf zone in a wave flume. They measured the flow velocities across a 1 :35 bottom slope with a fiber-optic laser-Doppler anemometer (LDA). The differences in turbulence intensity and velocity field between a spilling and a plunging breaker for a cnoidal wave were compared and discussed. However, they studied only one slope, i.e., $S = 1:35$, and their main interest was in the turbulence production below the trough level. In the field, the turbulent flow field caused by wave breaking is considered as the main factor affecting sediment transports; the transient velocity at the breaking point is the most decisive factor of the forces pounding on coastal structures. It is therefore important to predict the maximum particle velocity. The celerity at the crest of a breaking solitary wave on a slope was determined by Grilli *et al*. (1997):

$$C_b' = 0.466 + 2.58H_0' - 1.82(H_0')^2 \quad (25)$$

where C_b' is the crest celerity at breaking. They found that H_0' is the only significant factor affecting the variation of C_b' while the effect of slope is insignificant. However, Yasuda *et al*. (1997) have shown that both the largest velocity and/or acceleration within a wave are closely related to the breaker

type. In this study, forward difference is used to approximate the time derivative. The crest celerity at breaking thus determined is plotted in Fig. 11. The regression curve in Fig. 11 shows the relation between the wave celerity and the bottom slope, C_b and C_0 being the breaking wave and incident wave celerity, respectively.

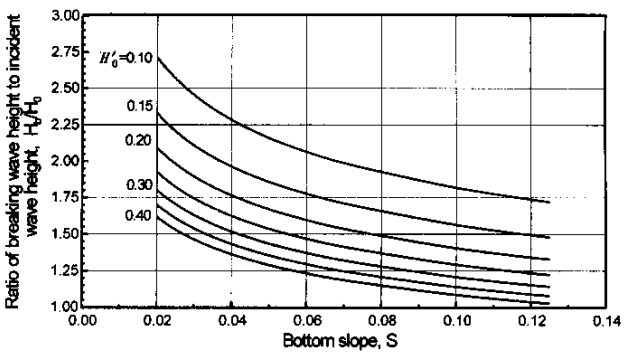

Fig. 10. Relation of wave height variations H_b/H_0 before and after breaking for various relative wave heights H_0' and slopes S.

When a wave approaches the surf zone, the wave period, T, remains constant while the wavelength, L, decreases, as a result, wave celerity $C(=L/T)$, as well as particle motions, will decrease due to shoaling. The ratio of the wave celerity at breaking to incident wave celerity that satisfies the condition of $C_b/C_0 < 1$ is given by:

$$\frac{C_b}{C_0} = 0.91384\exp(-0.07S_0). \tag{26}$$

By use of Eq. (26), the relation between the relative incident wave height H_0', the C_b/C_0 ratio, and the bottom slopes S can be determined, as shown in Fig. 12. It can be seen from Fig. 12 that, with the same bottom slope, increasing the value of H_0/h_0 will make the breaking point move away from the surf zone, i.e., the breaking point will be closer to the slope toe. Therefore, the values of C_b are much closer to C_0 than those for small H_0/h_0. As a result, C_b/C_0 increases along with the increase of H_0/h_0, and decreases with decreasing H_0/h_0. Yasuda *et al*. (1997) have also found that the maximum velocity of the high-speed area around a plunging jet is substantially larger than that of a spilling breaker. In the present study, since we have assumed that the cause of the breaker type is a significant factor for C_b/C_0, therefore in deriving Eq. (26), we have considered both the conditions of incident waves and bottom slopes, and used Fig. 3 as a reference for judging the breaker type. For the same incident wave condition, say, $H_0/h_0 = 0.2$, the breaker type will change from NB, PR, PL to SP as the bottom slope becomes milder, from $S = 0.12$ to 0.02 (1∶8 ~ 1∶50). A similar tendency can also be seen for the case where the slope remains constant but the incident wave height increases, e.g., $S = 1∶20$, $H_0/h_0 = 0.1 \sim 0.4$. From Fig. 12, it is concluded that the value of C_b/C_0 and its variation tendencies are closely related to the breaker type, which, in turn, is dictated by the condi-

tions of incident waves as well as the underlying bottom topographies.

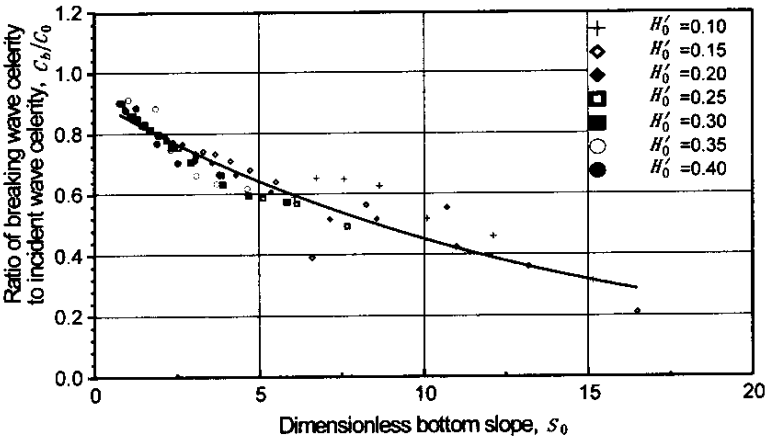

Fig. 11. Regression of breaking wave celerity C_b/C_0 ratio for solitary waves on slopes.

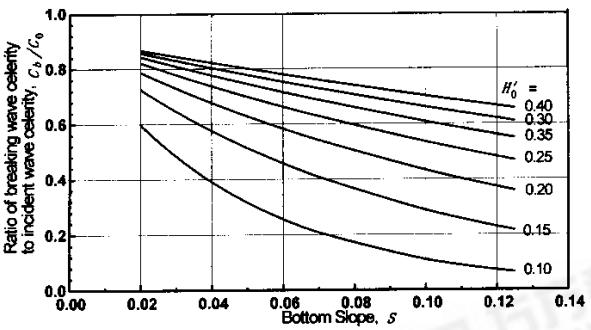

Fig. 12. Relation between relative incident wave height H_0', breaking wave celerity C_b/C_0 ratio, and bottom slope S.

4. Conclusions

In this paper, the process of breaking of solitary waves on slopes is studied with the boundary element method. Characteristics such as the breaking index, the wave height, the water depth, and the maximum particle velocity at the breaking point are studied. Our results show that these characteristics could be estimated by use of parameters such as the bottom slope S, the incident wave height H_0/h_0, and the wave steepness H_0/L_0. The results of simulation are summarized as follows:

(1) When $H_0/h_0 > 0.2$, our breaking criteria have values between those of Grilli *et al*. (1997) and Synolakis (1987). However, for $H_0/h_0 < 0.2$, our results suggest that breaking will occur on a slope milder than indicated by the other two previous results.

(2) For a large incident wave height and a steep slope, breaking occurs almost instantly without

rising too much in height. This is because the wave height will exceed the breaking criterion soon after it propagates on the slope.

(3) For waves on a mild slope the water depth at breaking, h_b/h_0, will be larger than that on a steep slope. The reason for this is that, waves on a gently sloping beach will have a much longer distance to travel than they do on a steep slope to have the same shoaling effect; if the inclination of the bottom slope is small, waves will have a longer distance to travel before breaking and thus will have a larger amplitude than those on a steep slope. Furthermore, the variation of h_b/h_0 is proportional to H_0' for waves on the same slope, i.e., breaking occurs earlier with a larger incident wave height.

(4) The ratio of breaker height to depth, H_b/h_b, is larger for small incident waves than for large waves. Furthermore, under the same wave conditions, the value of H_b/h_b is larger for a steep slope than for a mild slope.

(5) The ratio of the breaking wave height to the incident wave height, H_b/H_0, can be obtained as a function of the bottom slope, the relative water depth, and the dimensionless incident wave height. Its variation, which is larger for a small H_0/h_0 than for a large one, is 1.7 ~ 2.7 for the former, and 1.1 ~ 1.6 for the latter, respectively.

(6) Both the value of C_b/C_0 and its trend are closely related to the breaker type, which in turn, is determined by the conditions of the incident wave and the bottom topography, i.e., the slope.

Even though we have no experimental results to verify our numerical expressions at present, judging from the results of other researchers, the accuracy of these formulae seems to be confirmed.

References

Battjes, J.A., 1974. Surf Similarity, *Proceedings of the fourteenth Conference on Coastal Engineering*, 466 ~ 480.

Camfield, F.E. and Street, R.L., 1969. Shoaling of solitary waves on small slopes, *Journal of Waterway, Port, Coastal and Ocean Engineering*, ASCE, **95**(1): 1 ~ 22.

Camfield, F.E. and Street, R.L., 1968. The effects of bottom configuration on the deformation, breaking and run-up of solitary waves, *Proceedings of eleventh Conference on Coastal Engineering*, 173 ~ 189.

Chou, C.R. and Shih, R.S., 1996a. Numerical generation and propagation of periodical waves in time domain, *Coastal Engineering in Japan*, **39**(2): 111 ~ 127.

Chou, C.R. and Shih, R.S., 1996b. Generation and deformation of solitary waves, *China Ocean Engineering*, **10**(4): 419 ~ 432.

Chou, C.R. and Quyang, K., 1999a. The deformation of solitary waves on steep slopes, *Journal of the Chinese Institute of Engineers*, **22**(6): 805 ~ 812.

Chou, C.R. and Quyang, K., 1999b. Breaking of solitary waves on uniform slopes, *China Ocean Engineering*, **13**(4): 429 ~ 442.

Dommermuth, D.G. and Yue, D.K.P., 1987. Numerical simulations of nonlinear axisymmetric flows with a free surface, *Journal of Fluid Mechanics*, **178**, 195 ~ 219.

Dommermuth, D.G., Yue, D.K.P., Lin W.M., Rapp, R.J., Chan, E.S. and Melville, W.K., 1988. Deep-water plunging breakers: a comparison between potential theory and experiments, *Journal of Fluid Mechanics*, **189**, 423 ~ 442.

Galvin, C.J., 1968. Breaker classification on three laboratory beaches, *Journal of Geophysical Research*, **73**, 3651 ~ 3659.

Gotoh, H. and Sakai, T., 1999. Lagrangian simulation of breaking waves using particle method, *Coastal Engineering*

Journal, **41**(3): 303 ~ 326.

Grilli, S.T. and Subramanya, R., 1996. Numerical modeling of wave breaking induced by fixed or moving boundaries, *Computational Mechanic*, **17**(6): 374 ~ 391.

Grilli, S.T., Svendsen, I.A. and Subramanya, R., 1997. Breaking criterion and characteristics for solitary waves on slopes, *Journal of Waterway, Port, Coastal, and Ocean Engineering*, ASCE, **123**(3): 102 ~ 112.

Ippen, A.T. and Kulin, G.,1955. The shoaling and breaking of the solitary wave, *Proceedings of the Fifth Conference on Coastal Engineering*, 27 ~ 47.

Koshizuka, S., Nobe, A. and Oka, Y., 1998. Numerical analysis of breaking waves using the moving particle semi-implicit method, *International Journal for Numerical Methods in Fluids*, **26**, 751 ~ 769.

Street, R.L. and Camfield, F.E., 1966. Observations and experiments on solitary wave deformation, *Proceedings of the Tenth Conference on Coastal Engineering*, 284 ~ 301.

Saeki, H., Hanayasu, S., Ozaki, A. and Takagi, K., 1971. The shoaling and run-up height of the solitary wave, *Coastal Engineering in Japan*, **14**, 25 ~ 42.

Synolakis, C.E., 1987. The runup of solitary waves, *Journal of Fluid Mechanics*, **185**, 523 ~ 545.

Ting, F.C.K. and Kirby, J.T., 1994. Observation of undertow and turbulence in a laboratory surf zone, *Coastal Engineering*, **24**, 51 ~ 80.

Trizna, D.B., Tang, S. and Wu, J., 1999. On extreme spatial variations of surface slope for a spilling breaking water wave, *Journal of Atmospheric and Oceanic Technology*, **16**, 92 ~ 95.

Tsusaka, N., 1983. Boundary element analysis of nonlinear water wave problem, *International Journal for Numerical Method in Engineering*, **19**, 953 ~ 970.

Weggel, J.R., 1972. Maximum breaker height, *Journal of Waterway, Port, Coastal, and Ocean Engineering*, ASCE, **98**(5): 529 ~ 548.

Yasuda, T., Mutsuda, H. and Mizutani, N., 1997. Kinematics of overturning solitary waves and their relations to breaker types, *Coastal Engineering*, **29**, 317 ~ 346.